Chapter 5
Creep and Irradiation Effects in Reactor Vessel Internals

Dmytro Breslavsky and Oksana Tatarinova

Abstract The paper is devoted to the presentation of the calculation method for determining the stress-strain state and long-term strength of reactor vessel internals (RVI) and the description of the results obtained with its help. The method is based on a complete mathematical formulation of the boundary- initial value problems of creep accompanied by irradiation effects. Deformation and damage accumulation caused by irradiation effects in the material when interacting with the effects caused by thermal creep, can significantly limit the safe operation of RVI. Elastic, thermoelastic, thermal and irradiation creep, irradiation swelling strains, creep damage and fracture are considered. The numerical solution of the boundary value problems is performed by the FEM, and the initial value problems are solved by time integration. To estimate cyclic deformation and fracture, the procedures of asymptotic methods and averaging over cycle periods are used. As an examples of the use of this calculation method, the results of creep modelling of fuel element, T-joint of tubes and notched plates are given. The issues of interaction of stresses, strains and damages of different nature under complex stress state are discussed.

5.1 Introduction

Creep accompanied by the accumulation of hidden damage is a complex phenomenon. In nuclear reactor vessel internals (RVI) it is also accompanied by effects associated with the action of irradiation. Deformation and damage accumulation caused by irradiation effects in the material, such as irradiation creep, irradiation swelling, when interacting with the effects caused by thermal creep, can significantly limit the safe operation of RVI [1, 2].

Dmytro Breslavsky · Oksana Tatarinova
Department of Computer Modelling of Processes and Systems, National Technical University "Kharkiv Polytechnic Institute", UKR-61002, Kharkiv, Ukraine,
e-mail: dmytro.breslavsky@khpi.edu.ua, ok.tatarinova@gmail.com

© The Author(s), under exclusive license to Springer Nature Switzerland AG 2023
H. Altenbach and K. Naumenko (eds.), *Creep in Structures VI*,
Advanced Structured Materials 194, https://doi.org/10.1007/978-3-031-39070-8_5

Creep, which occurs as a result of radiation and is accompanied by high plasticity of fuel and structural materials, is called irradiation creep. It is known that the rate of irradiation creep can be several times higher than the rate of creep of the same material at the same stress level [3–5]. In order to distinguish the mechanisms of creep that occurs during radiation exposure and under the action of only temperature-force fields, the term 'thermal' creep will be used for the latter.

Radiation exposure under conditions of long-term operation leads to another effect - irradiation swelling, which is volumetric instability caused by the formation of pores and bubbles in the material and the accumulation of inert gas. At the same time, the increase in volume is accompanied by a decrease in the density of the material. Irradiation swelling limits the operational properties of fuel rods and other elements of the reactor during operation [4].

Like as in traditional creep-damage studies [6], the role of numerical simulation of the RVI is no less important. Experimental studies are not only very expensive due to their duration, but also require, firstly, unique laboratory equipment, and, secondly, are associated with the need to observe strict safety measures due to possible irradiation damage. If it is still possible to conduct experiments with a uniaxial stress state, which are absolutely necessary to determine the properties of the material under radiation exposure, then there are very few data on deformation measurements under a complex stress state.

As with the numerical simulation of creep and fracture of structural elements, FEM approaches are used to analyze the stress-strain state of RVI using both standard engineering software such as ANSYS, ABAQUS [7–9], and specially developed ones [10–12]. The basis for numerical modeling of the deformation processes in structural elements subjected to the joint action of thermal-force and radiation fields is the use of the hypothesis of strains additivity (in most cases, the problems are solved using the Lagrange approach). Constitutive equations are formulated for each physically nonlinear component of the total strain tensor (plasticity, thermal and irradiation creep, irradiation swelling, etc.). It is clear that the adequacy and accuracy of numerical solutions depends on their adequacy. If classical, proven constitutive equations are used for plasticity and creep strains description, then the predicting the irradiation swelling strains, which are often quite significant and dangerous [4, 5], is still far from classical completion. Irradiation swelling strains have a volumetric nature, and their description in Solid Mechanics is carried out using the equations corresponding, for example, to the one used in the calculation of thermal strains. When formulating the functional dependence used to describe the process of strain accumulation during irradiation swelling, information is used regarding its dependence on the integral neutron flux, fluency or accumulated radiation dose, temperature, and time. However, further such dependencies are built directly using experimental distributions, which are processed by the method of least squares [13]. Unfortunately, in most publications, dependencies are formulated precisely for the expressions of swelling strains, while for the correct formulation of the boundary- initial value problems, a formulation in rates is required. Reformulation of these state equations obtained for the strain values to an incremental form can lead to significant inaccuracies in calculations [14].

The irradiation creep of metals and alloys is often found to be described by linear dependencies on the applied stresses [4]. Sometimes, when processing the results of experimental studies, it is possible to formulate the dependence of the irradiation creep function on swelling [5], but such equations still require further verification.

As shown by experimental and numerical studies [1–5], the addition of radiation exposure significantly, quantitatively and qualitatively, changes the characteristics of creep processes in structural elements. As for hidden damage accumulation processes, experimental data in most cases also indicate their intensification when radiation exposure is added. Damage calculations of RVI elements using Continuum Damage Mechanics (CDM) approaches are extremely few. This is primarily due to the difficulty of obtaining experimental data on long-term behavior during radiation exposure, and possibly to the lack of appropriate units in many FE software complexes.

Due to the fact that the main structural materials of the active zone of nuclear reactors were steels and alloys, which in most cases did not show significant anisotropy of physical and mechanical properties, the calculations were carried out assuming isotropy of deformation properties and accumulation of damage. By the way, a number of light alloys are used for the manufacture of RVI elements, which are characterized by significant anisotropy of both classical physical and mechanical properties [6] and deformation during radiation exposure [15–17]. Their numerical modeling requires the verification and formulation of more complex constitutive equations, and the use of tensor models to predict damage accumulation.

The operation of nuclear reactors is not constant over time, they are periodically shut down, and many RVI elements are subjected to cyclical varying in temperature and pressure. This mode of their work is associated with the need to reformulate the boundary initial value problems with the involvement of new constitutive equations, which reflect the influence of cyclic loading, heating-cooling, and irradiation on creep and damage accumulation. Investigations in this direction are just beginning to be carried out, modeling of non-uniform loading is the subject of few publications [18, 19]. Yang et al. [19] demonstrate the results of calculations of irradiation swelling were carried out using ANSYS procedures, in which physical and mechanical properties were determined as functions of time. Dubyk et al. [18] also used the developed additional software for the ANSYS to model the reactor baffle taking into account shutdowns.

This paper is devoted to the presentation of the main approaches, methods and constitutive equations used for numerical modeling of creep-damage processes in RVI elements made of materials that exhibit isotropic or anisotropic properties and can be cyclically loaded. The presented numerical examples demonstrate the capabilities of the calculation method for the purpose of determining the laws of deformation and fracture.

5.2 Problem Statement and Description of Solution Approaches.

Let us consider a solid with a volume V fixed on a part of the surface S_1 and loaded with volume forces $\boldsymbol{f}$ and traction $\boldsymbol{P}$ and on a part of the surface S_2 (Fig. 5.1). In the coordinate system $\boldsymbol{x} = (x_1, x_2, x_3)$ the motion of the continuum of material points will be described by the displacement vector $\mathbf{u}$, tensors of stresses $\boldsymbol{\sigma} = \sigma(x_i, t)$, $\sigma_{ij} = \sigma_{ji}$ and strains $\boldsymbol{\varepsilon} = \boldsymbol{\varepsilon}(x_i, t), \varepsilon_{ij} = \varepsilon_{ji}, (i, j = 1, 2, 3)$, which are functions of coordinates and time t. Irreversible creep strains are represented by a tensor $\boldsymbol{c} = \boldsymbol{c}(x_i, t), c_{ij} = c_{ji}$. The tensor connection for them with the stress tensor components and time is determined by the accepted constitutive equations.

An inhomogeneous temperature field $T(x_i, t)$ acts on the solid, the effect of which causes thermal strains $\boldsymbol{\varepsilon}^{\mathrm{T}} = \boldsymbol{\varepsilon}^{\mathrm{T}}(x_i, t)$, with components $\varepsilon^{\mathrm{T}}_{ij} = \varepsilon^{\mathrm{T}}_{ji}$. The components of the total initial strain e_{ij} consist of elastic e^{e}_{ij} and thermoelastic strains $\varepsilon^{\mathrm{T}}_{ij}$. The presence of radiation exposure leads to the development of irradiation creep and irradiation swelling strains with components c^{r}_{ij} and $\varepsilon^{\mathrm{sw}}_{ij}$, respectively.

Let us specify the nature of the external load field. Acting external forces can be divided into two components - main and oscillating action. To the first we include volume forces $\boldsymbol{f}(\boldsymbol{x}, t), \boldsymbol{x} \in V$, and the part of traction $\boldsymbol{P}^0(\boldsymbol{x}, t), \boldsymbol{x} \in S_2$, which slowly varies over time or remain unchanged. The second part include tractions and forces that change over time according to the harmonic law with amplitude P^{a}_i and period T_{c}

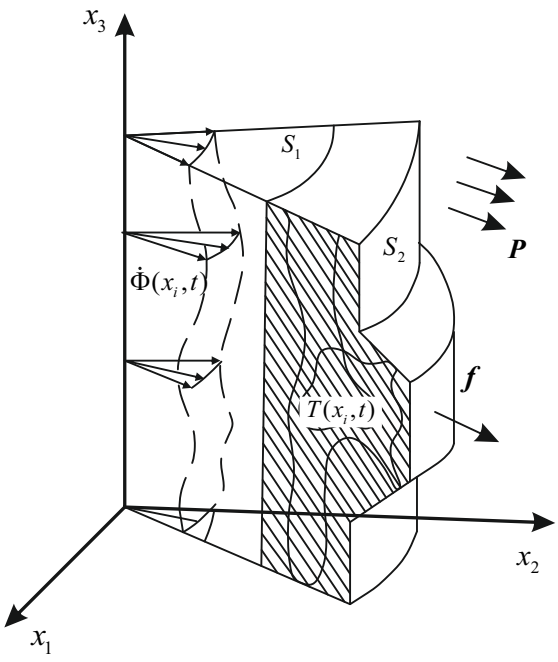

Fig. 5.1 Solid in thermal-force and radiation fields.

$$P_i = P_i^0 + P_i^{\mathrm{a}} \sin \frac{2\pi}{T_{\mathrm{c}}}$$

In the assumptions formulated above, the mathematical formulation of the boundary - initial value problem of the creep of solids under the action of periodically varying loads can be represented by the following system of equations:

$$\sigma_{ij,j} + f_i = \rho \ddot{u}_i, \quad \sigma_{ij} n_j = P_i, \qquad x_i \in S_2, \tag{5.1}$$

$$\varepsilon_{ij} = \frac{1}{2}\left(u_{i,j} + u_{j,i} + u_{k,i} u_{k,j}\right), \qquad x_i \in V, \quad u_i|_{S_1} = \bar{u}_i, x_i \in S_1,$$

$$\varepsilon_{ij} = e_{ij} + c_{ij} + c_{ij}^{\mathrm{r}} + \varepsilon_{ij}^{\mathrm{sw}}, \qquad e_{ij} = e_{ij}^{\mathrm{e}} + \varepsilon_{ij}^{\mathrm{T}},$$

$$\sigma_{ij} = D_{ijkl}\left(e_{kl} - c_{kl} - c_{kl}^{\mathrm{r}} - \varepsilon_{kl}^{\mathrm{sw}}\right),$$

$$u_i(x,0) = c_{ij}(x,0) = c_{ij}^{\mathrm{r}}(x,0) = \varepsilon_{ij}^{\mathrm{sw}}(x,0) = 0.$$

where ρ is the mass density; $\mathbf{n}$ is unit normal to the solid boundary; D_{ijkl} are the components of the elastic properties tensor, $i = 1,2,3, \bar{u}_i$ are the known displacement values in the surface part S_1, which do not vary in time.

To determine the limits of the study, we will introduce several assumptions. Due to the fact that we are considering structural elements in which large displacements and strains are prohibited by their purpose, we will limit ourselves to the Lagrange approach. We will consider quasi-static load processes, which is due to the fact that during design, a search is made for the eigen frequencies of the system and it is verified that the frequencies of its forced oscillations are far from them. In connection with this, we will neglect the term corresponding to inertial forces in the equation of motion, system (5.1). The hypothesis of strains additivity is applied. In the case when processes characterized by a coupling between irradiation creep and swelling strains take place, it is possible to postulate the existence of the hypothesis of additivity over an infinitesimally small interval of time. But such processes will not be considered.

When considering the processes of cyclic varying the stresses due to the fact that such problems for non-isotropic solids are just beginning to be investigated and simple qualitative conclusions are needed, we will limit ourselves to the case of stress varying according to a harmonic law with a low frequency. Such a case corresponds to a varying of a pressure from a gas flow and is considered in [10] for the isotropic properties of the material. To solve the problem, we will use the approaches of the method of many time scales and averaging over the period of varying stresses. At the same time, two systems of equations are obtained, one of which describes the deformation of a solid under the influence of a thermal-force field and radiation exposure and the action of only time-invariant load components, and the other is analogous to the problem of quasi-static elastic loading in a cycle. The systems are connected by the constitutive equations, which will be given below, in the Sect. 5.3. The used approach of reducing the cyclic loading process to the equivalent quasi-static one is described in [20–22] and also presented by the authors in another paper of this symposium. The approaches developed by the authors use FEM for solving boundary-value problems, and finite difference approaches for solving

initial problems in time. To describe the development of a macrodefect (crack), which occurs after the completion of hidden damage accumulation, a process based on a series of reformulated boundary-initial value problems is used. In them, the initial conditions are determined by the distributions of components of the stress-strain state and damage parameter in finite elements acquired before the completion of the next hidden damage accumulation in next finite element, and the boundary conditions are determined by the current configuration of the considered structural element, taking into account its destroyed parts. A description of the method and corresponding algorithms can be found in [23, 24]. In addition to Solid Mechanics problems, the ability to determine temperature fields in stationary and non-stationary heat conduction problems is also implemented. A description of the method and software can be found in [25, 26]. During the last decades, experimental verification of the method, constitutive equations, and implemented software under uniaxial and complex stress states was performed, some results and references are presented in [21, 22, 24, 26].

5.3 Constitutive Equations

To demonstrate the capabilities of the calculation method, we will consider two versions of the constitutive equations: first for describing the behavior of materials with isotropic properties as well as second one for non-isotropic (in this case, transversal isotropic) properties of deformation and accumulation of hidden damage.

5.3.1 Materials with Isotropy of Properties

Here we use the equations only for static loading and irradiation effects. Cyclic behaviour of structures made from materials with isotropic properties is described by appropriate equations and analyzed in [21, 22, 24, 26].

The description of thermal creep and the damage accumulation associated with it will be performed using the following equations:

$$\dot{\boldsymbol{c}} = \frac{3}{2} b \frac{\sigma_{\mathrm{vM}}^{n-1}}{(1-\omega)^l} \left[\tilde{B}\right] \boldsymbol{s} \tag{5.2}$$

$$\dot{\omega} = d \frac{\sigma_{\mathrm{e}}^{r}}{(1-\omega)^l} \tag{5.3}$$

where $\boldsymbol{s} = \boldsymbol{s}(x_i, t)$ is the deviator of stress tensor, ω is scalar damage parameter introduced by Kachanov-Rabotnov approach, σ_{vM}, σ_{e} are von Mises equivalent stress and equivalent stress is obtained by use of fracture criterion which appropriate for considered material [6]; b, n, d, r, l are the material constants obtained only from experiments on creep and long-term strength under static load and constant

temperature values on standard samples under tension. Here we will limit ourselves to cases of either constant temperature over the entire volume of the structural element, or moderate temperature changes, when thermo-physical and long-term physical and mechanical properties can be considered unchanged.

The irradiation swelling strain $\varepsilon_{ij}^{\mathrm{sw}}$ is volumetric, so $\varepsilon_{ij}^{\mathrm{sw}} = 0$ at $i \neq j$. In general case it describes by function S_Φ, which depends upon neutron fluency Φ, time t and temperature T:

$$\dot{\varepsilon}_{ij}^{\mathrm{sw}} = \frac{1}{3}\dot{S}_\Phi\left(\dot{\Phi}, t, T\right)\delta_{ij} \tag{5.4}$$

As noted, the expression for swelling function S_Φ is often determined numerically using approximation procedures. For example, for steel type 0.08 % C, 16 % Cr, 11 % Ni, Mn 3%, 0,2-0.4 % Nb for the neutron fluence range $\dot{\Phi}$= 4..6 $10 \cdot 19$ neutron/m^{2}s and temperature values 458-790 K it was determined as the following dependence [10]:

$$\dot{S_\Phi} = A_1\beta_1\left(\alpha_1\dot{\Phi}\right)^{\beta_1} t^{\beta_1 - 1}\exp\left(0.0235T - \frac{83.5}{T-630} - \frac{1782}{980-T}\right), \tag{5.5}$$

where $A_1 = 5.33 \cdot 10^{-9}, \beta_1 = 0.19 + 1.63 \cdot 10^{-3}T, \alpha_1\dot{\Phi} = 9.37 \cdot 10^{-3}$ dpa/h. Irradiation creep strains will be calculated using the linear dependence of the strain rate on stresses [4, 5]:

$$\dot{\boldsymbol{c}} = \frac{3}{2}b_{\mathrm{rc}}\sigma_{\mathrm{vM}}[\tilde{B}]\boldsymbol{s} \tag{5.6}$$

where b_{rc} is the material constant for considered temperature range.

5.3.2 Materials with Transversal Isotropy of Properties

As is known [6], at elevated temperatures, even materials that are isotropic during elastic deformation, can exhibit non-isotropic properties of creep and hidden damage. Let us consider the constitutive equations proposed by Morachkovsky for materials with transversely isotropic properties of creep and damage [27] and modified in [28] for the case of cyclic loading. We consider the case of a quasi-static harmonic load with frequencies in the range of 1. . . 3 Hz (that is, forced oscillations that occur far from the eigen frequencies of the structural element during gas flow oscillations. At the same time, the contribution of inertial forces is neglected). The used equations are as follows:

$$\dot{\boldsymbol{c}} = \tilde{B}H(A)\frac{\sigma_{\mathrm{v}}^{m-1}}{(1-\eta)^m}[\bar{B}]\boldsymbol{\sigma}, \qquad A = \frac{\sigma_{\mathrm{v}}^a}{\sigma_{\mathrm{v}}} \tag{5.7}$$

$$\dot{\boldsymbol{\omega}} = d_{1111}^{p/2}K(A_D)\frac{\sigma_D^{p-2}}{(1-\eta)^{p+s-1}}[\bar{D}]\boldsymbol{\sigma}, \qquad \dot{\boldsymbol{\eta}} = d_{1111}^{p/2}K(A_D)\frac{\sigma_D^p}{(1-\eta)^{p+s}}, \tag{5.8}$$

$$\eta(0) = 0, \quad \eta(t_*) = 1, \quad A_d = \frac{\sigma_D^a}{\sigma_D}$$

where $\boldsymbol{\omega}$ is the damage tensor. $\sigma_{\mathrm{v}} = \boldsymbol{\sigma}^T[\bar{B}]\boldsymbol{\sigma}$, $\sigma_D = \boldsymbol{\sigma}^T[\bar{D}]\boldsymbol{\sigma}$ are the equivalent stresses which are the joint invariants of stress tensors and tensors of material constants; $\eta = \eta(t)$t is scalar damage measure. The index a denotes the equivalent stresses calculated by use the amplitude components of the stress tensor under cyclic loading. At the time t_* of the finishing the hidden damage accumulation process $\eta(t_*)$=1. Matrix $[\bar{B}]$ contains the components of the material creep properties tensor b_{ijkl}:

$$[\bar{B}] = \begin{bmatrix} 1 & \beta_{12} & 0 \\ \beta_{12} & \beta_2 & 0 \\ 0 & 0 & 4\beta \end{bmatrix}, \quad \beta_{12} = -\frac{1}{2}b_{1111}, \quad \beta_{22} = \frac{b_{2222}}{b_{1111}}, \quad 4\beta = \frac{b_{1212}}{b_{1111}} \tag{5.9}$$

Matrix $[\bar{D}]$ contains the components of the material creep damage properties tensor d_{ijkl} :

$$[\bar{D}] = \begin{bmatrix} 1 & \delta_{12} & 0 \\ \delta_{12} & \delta_2 & 0 \\ 0 & 0 & 4\delta \end{bmatrix}, \quad \delta_{12} = -\frac{1}{2}d_{1111}, \quad \delta_{22} = \frac{d_{2222}}{d_{1111}}, 4\delta = \frac{d_{1212}}{d_{1111}} \tag{5.10}$$

The functions $H(A)$ and $K(A_D)$ are obtained after expanding the functions of the creep strain and the damage measure into an asymptotic series on a small parameter

$$\mu = \frac{T_c}{t}$$

in two time scales (slow t and fast $\xi = \tau/T$, $\tau = t/\mu$):

$$c \cong c^0(t) + \mu c^1(\xi), \qquad \eta \cong \eta^0(t) + \mu\eta^1(\xi), \tag{5.11}$$

where T_{c} is the period of cyclic load; $c_0(t)$, $\eta_0(t)$t), $c_1(t)$, $\eta_1(t)$ are the functions corresponding to the main creep and damage processes in slow (0) and fast (1) time scales. The expressions of these functions can be found in [20, 22, 26]. Then, with the help of the averaging procedure over the period T_{c}, constitutive equations (5.7) - (5.8) are obtained. At the same time, the main system of equations (5.1) remains unchanged, but now it describes the deformation motion of its points already in the main, slow time. The derivation of the equations is described in more detail in [20, 22, 26] .

The components of the tensors b_{ijkl} and d_{ijkl} are determined by the results of experiments on the creep and long term strength of samples cut from the material in three directions. In the case of sheet materials produced by rolling, these are the directions along, across the rolling and at an angle of 45° to them. $\tilde{B}, m, p, s$ are the constants determined experimentally.

Next, we will consider the equation for determining the components of the irradiation swelling strain tensor. In the case of anisotropy of the swelling properties, we write

$$\dot{\varepsilon}_{ij}^{\mathrm{sw}} = \frac{1}{3}\beta_{ij}\dot{S}_{\Phi}\left(\dot{\Phi}, t, T\right)\delta_{ij} \tag{5.12}$$

where β_{ij} are the coefficients reflecting the effect of anisotropy on the swelling process. Due to the information about the isotropic nature of the irradiation creep [29], we will describe it by Eq. (5.6).

5.4 Deformation, Damage Accumulation and Fracture in RVI

Let us consider examples of stress-strain state, damage accumulation and fracture modeling, obtained by use of 2D and 3D models of RVI structural elements.

5.4.1 Creep of T-joint of Tubes

As a first example, let's consider the results of numerical modeling of the processes of thermal creep and irradiation swelling of the T-joint of the cooling tubes from system of the reactor core (Fig. 5.2) [26]. The following dimensions are used: inner radius 50 mm, outer radius 100 mm. For the operational temperature range, the following data are accepted: Young's modulus $E = 1.55 \cdot 10^5$ MPa , Poisson's ratio $\nu = 0.3$, coefficient of thermal expansion $\alpha = 14.7 \cdot 10^{-6}(C^{\circ})^{-1}$, yield limit $\sigma_{\mathrm{y}} = 650$ MPa, ultimate strength $\sigma_{\mathrm{u}} = 980$ MPa.

Let us use the isotropic material model (5.2) without taking into account the damage of the material. The creep constants have the following values:

$$b = 3.6 \cdot 10^{-19.9}\mathrm{MPa}^{-n}/\mathrm{h}, \qquad n = 4.9.$$

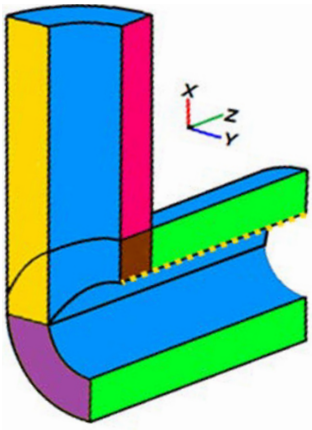

Fig. 5.2 Model of T-joint.

The T-joint is loaded with a uniformly distributed internal pressure of 120 MPa, the temperature field has a steady character and is characterized by a logarithmic distribution of temperatures in the radial direction, at the outer and inner radii temperature values of 740 K and 752 K are maintained, respectively. The rate of the integral flux function is given in the form of the experimentally obtained Eq. (5.5).

The calculations were carried out in the general 3D statement, due to the joint's symmetry, one half of it was considered as a FE model (Fig. 5.2). In this figure surfaces for which different formulations of boundary conditions symmetry were used are marked with different colors. Calculations were made for a time of 10,000 h. Figure 5.3 shows the varying of the maximum von Mises stress, which obtained in the stress concentrator (situated at the transition zone between the tubes). Curve 1 is built only for the creep problem as well as curve 2 presents the result of combined problem of creep and irradiation swelling. Figure 5.4 shows the distributions of von Mises stress in the cross-section of the T-joint also when solving the separate problem of thermal creep (a) and the combined problem of creep and irradiation swelling (b).

Thermal creep of tubes is well studied, it is characterized by significant redistribution of stresses with their general relaxation [21, 30]. Curve 1 of Fig. 5.3 also confirms this property of creep under the action of internal pressure. But adding to the analysis the effect of radiation exposure, which leads to the development of swelling, qualitatively changes the nature of the change in the stress state. Comparing Fig. 5.4 a) and b) we can see that the stress levels differ from 150 MPa for the maximum and 80 MPa for the minimum values. Due to the effect of swelling strains, the stress level increases, and due to stress relaxation during creep, it mainly decreases. Obviously, it is possible to find such a value of internal pressure that will compensate the effect of swelling. A more detailed description of the results can be found in [26].

5.4.2 *Damage Accumulation and Fracture of Reactor Fuel Element*

It is known [31] that the facts of the fracture of fuel elements claddings are the most dangerous factor from the point of view of ensuring their durability. At the same time,

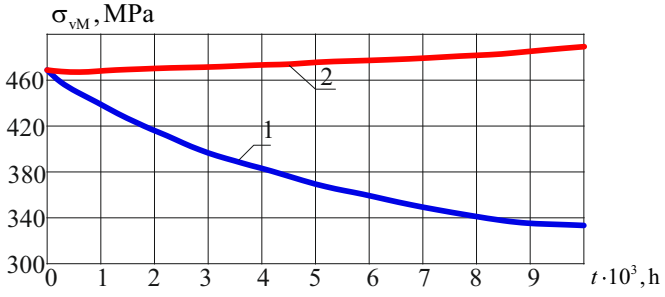

Fig. 5.3: Evolution of maximum von Mises stress in T-joint.

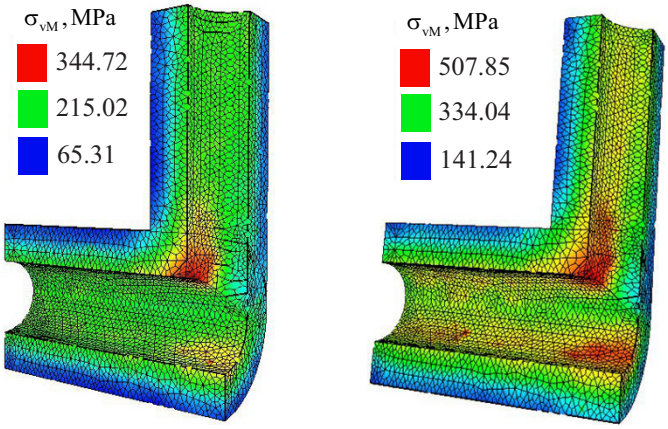

Fig. 5.4: Distribution of the von Mises stresses in the T-joint. a) thermal creep, b) thermal creep and irradiation swelling.

the fracture can go together - not only in the cladding, but also in the nuclear fuel. The resulting crack causes rapid loss the operability in both elements. As an example, Fig. 5.5 [31] shows the appearance of a crack developing in the fuel cladding and in the fuel itself. During the operation of fuel rods, their stress-strain state is determined by two main factors - the internal pressure of the gas gap and the mechanical load that occurs as a result of bending in the spaces between the tube boards [4].

Let us analyze the process of fuel rod fracture. It can take place under the condition that the gas gap is already absent due to the irreversible deformation of the fuel. In this regard, a calculation scheme without a gap between the fuel and the fuel cladding is involved in the simulation.

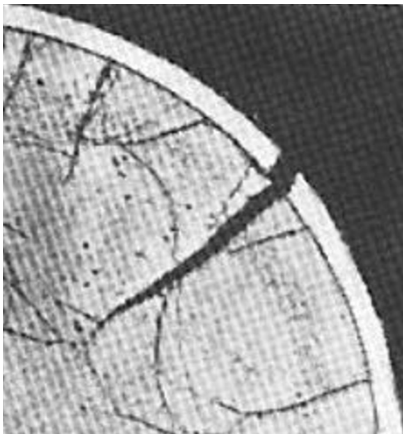

Fig. 5.5 Fracture of nuclear fuel together with the fuel cladding [B.R.T. Frost. Nuclear Fuel Elements. Oxford: Pergamon Press, 1982]

To simulate the bending of the fuel rod in its cross-section, the following calculation model was built. At the first stage, fuel rod is considered as a hinged beam during bending. According to the approaches of the theory of beam bending, the stress state was determined. The mid-length cross-section of the fuel rod is considered. The determined stresses were applied at the points of the cross-section in 2D model (plane strain scheme) of the fuel rod with a maximum value of static load on the surfaces of 25 MPa. Due to the symmetry of the stress state, a model for one half of the section was used.

In the calculations, it is assumed that the cladding is made of IN100 alloy. The creep-damage constants of this material were obtained:

$$b = 3.43 \cdot 10^{-29} (\text{MPa})^{-n}/\text{h}, n = 9.7, d = 7.5 \cdot 10^{-15} (\text{MPa})^{-r}/\text{h}, r = 5.2, l = 15.$$

Material parameters for the fuel material:

$$b = 1.25 \cdot 10^{-7} (\text{MPa})^{-n}/\text{h}, n = l = r = 3, d = 3.125 \cdot 10^{-7} (\text{MPa})^{-r}/\text{h}$$

were obtained by use experimental data [26].

We present the results of numerical simulation of creep, damage accumulation and subsequent fracture development for a cross-section of fuel rod under constant bending by the load linearly increasing up to 25 MPa on the surface of the cladding. According to the simulation data, it was established that after 318,443 h of creep, accompanied by hidden damage accumulation, a macrodefect appears on the outer surface of the fuel cladding (Fig. 5.6). Its material is destroyed simultaneously in several finite elements. Further, the development of the macrodefect proceeds quite quickly, within 0.001 h (3 s) it spreads to the fuel area (Fig. 5.7). After a few more seconds, the complete fracture of the fuel in the cross-section occurs [26].

Analysis of the obtained numerical results shows that the existence of a macrodefect in the fuel rod under consideration is limited to a few seconds. This means that for the considered material composition the assessment of its long-term strength can be performed only by calculating the processes of damage accumulation, without the involvement of a specialized software tool for simulation of fracture.

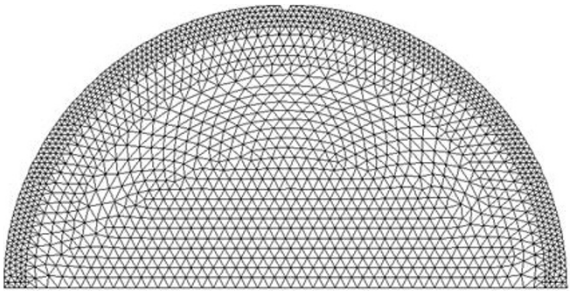

Fig. 5.6 View of the fuel rod cross-section model at the end of the hidden damage accumulation, $t = 318,443$ h

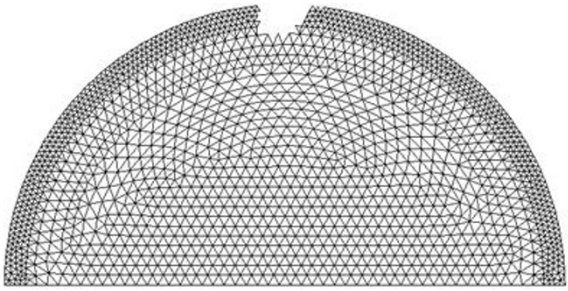

Fig. 5.7 View of the fuel rod cross-section model during fracture process at the time $t = 318,444$ h.

5.4.3 *Transversal-Isotropic Creep-Damage Behaviour of Aluminium Notched Plate*

The next example is related to the demonstration of the behavior of a representative of light alloys, which present class of materials exhibiting anisotropy of properties [15]. Consider the processes of thermal and irradiation creep, accompanied by the accumulation of hidden damage and the growth of irradiation swelling strains in a plate with side circular notches. Plate material is aluminum alloy type 2024. This problem is classic for the creep theory, but it is also of practical importance for some elements of RVI fasteners.

The plate is loaded by traction of 1 MPa, it is in a non-uniform temperature field (230 – 280°C and under the action of radiation exposure. The material of the plate is characterized by significant anisotropy of creep properties and accumulation of hidden damage. The constants for the constitutive equations (5.7), (5.8) for this alloy are given in [32]. They are equal to:

$$b_{1111} = 6.669 \cdot 10^{-5}, b_{1122} = -3.334 \cdot 10^{-5}, (\text{MPa})^{(-2n/(n+1))}/\text{h}^{(2/(n+1))},$$

$$b_{2222} = 7.653 \cdot 10^{-5}, b_{1212} = 5.332 \cdot 10^{-5}, (\text{MPa})^{(-2n/(n+1))}/\text{h}^{(2/(n+1))},$$

$$d_{1111} = 1.159 \cdot 10^{-5}, d_{1122} = -5.794 \cdot 10^{-6}, (\text{MPa})^{-2}/\text{h}^{2/p},$$

$$d_{2222} = 1.385 \cdot 10^{-5}, d_{1212} = 9.437 \cdot 10^{-6}, (\text{MPa})^{-2}/\text{h}^{2/p},$$

$$m = p = 3.4, s = 0.$$

As noted in the Introduction, the description of irradiation swelling processes due to the complexity of experimental measurements during radiation exposure is a difficult task. Complete data for aluminum alloys, from which it is possible to construct an equation of state, are very scarce. In this regard, we will use the data given in various publications [15–17, 29] in order to build a qualitatively reliable model of type (5.4). To construct an equation for describing the strains of irradiation swelling, which are dependent on the values of temperature T and neutron fluency F, we apply exponential dependencies:

$$\dot{\varepsilon}_{ij}^{\mathrm{sw}} = \frac{1}{3}\beta_{ij}\exp\left(-\frac{Q_{\mathrm{T}}}{T}\right)\exp\left(-\frac{F_{\mathrm{F}}}{F_1+10F}\right)\delta_{ij}, \qquad Q_{\mathrm{T}} = \frac{U_{\mathrm{T}}}{R}, \tag{5.13}$$

where U_{T} is the value of activation energy for irradiation swelling process,

$$Q_{\mathrm{T}} = 6968.8\mathrm{K}, F_{\mathrm{F}} = -5.92\cdot 10^{26}\mathrm{neutron/m}^2, F_1 = 7\cdot 10^{26}\mathrm{neutron/m}^2.$$

The value of the threshold time for the beginning of the development of the irradiation swelling process is 15,000 h. Using data from [29, 33] for the temperature range under consideration, the value of the radiation creep constant was obtained:

$$b_{\mathrm{rc}} = 3\cdot 10^{-6}\mathrm{MPa}^{-1}/\mathrm{h}.$$

Due to the symmetry of the plate with two side notches, calculations were made for its fourth part. The results of the calculations in the form of distributions of temperatures (Fig. 5.8 a), damage measure and von Mises strains are presented in Figs. 5.8 - 5.12.

The cycle of calculation studies included the following variants of modeling: only thermal creep and damage of the plate without the influence of radiation exposure (variant 0, Figs. 5.8 b) and 5.9 a); thermal and irradiation creep and damage of the plate without the influence of irradiation swelling (variant 1, Fig. 5.11 a); thermal and irradiation creep and damage, taking into account the effect of isotropy of irradiation swelling (variant 2, $\beta_{ij} = 1$, Figs. 5.9 b) and 5.11 b) and in cases of transversal isotropy (variant 21 ($\beta_{11} = 2$, $\beta_{22} = 0.5$, Figs. 5.10 a) and 5.12a) and variant 22 ($\beta_{11} = 0.5$, $\beta_{22} = 2$, Figs. 5.10 b) and 5.12 b).

We will present the obtained values of the time until the completion of hidden damage accumulation: variant 0: $t_* = 50175$ h; variant 1: $t_* = 37869$ h; variant 2: $t_* = 37728$ h; variant 21: $t_* = 50727$ h; variant 22: $t_* = 33864$ h. As can be seen, the

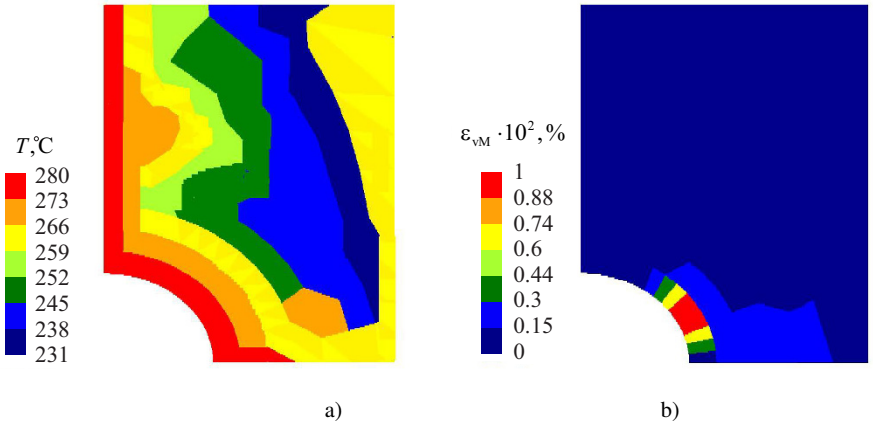

Fig. 5.8: Distribution of temperature a) and von Mises strains, b) in an aluminum plate with a notch, thermal creep, t_*=50175 h, static loading.

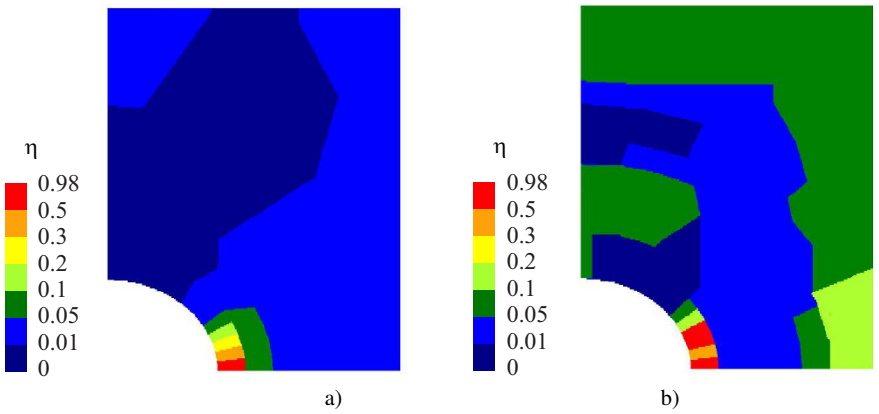

Fig. 5.9: Distribution of the damage measure in an aluminum plate with a notch a) thermal creep $t_* = 50175$ h, b) thermal, irradiation creep and irradiation swelling, $t_* = 37728$ h.

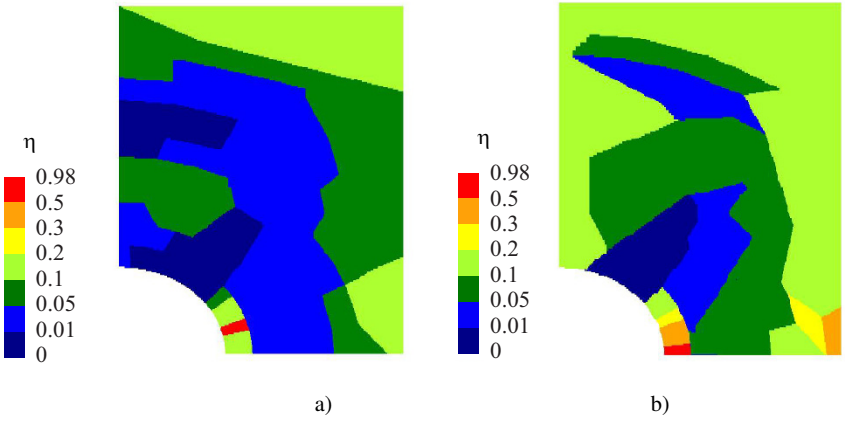

Fig. 5.10: Distribution of the damage measure in an aluminum plate with a notch. Thermal, irradiation creep and anisotropic irradiation swelling a) variant 21, $t_* = 50727$ h, b), variant 22, $t_* = 33864$ h.

addition of another process of creep (irradiation, variant 1) significantly intensifies the process of stress redistribution and, thanks to this, an increase in damage rate, which lead to more fast fracture. Adding isotropic irradiation swelling to the analysis (variant 2) leads to a further, but insignificant, reduction in the time to completion of hidden damage accumulation. Finally, the anisotropy of swelling properties can both significantly, by 4000 h, reduce the time t_* obtained in the isotropic analysis (variant 22), and significantly increase it, even in comparison with purely thermal processes (variant 21).

The analysis of the distribution of hidden damage in the case of not taking into account the influence of radiation exposure (variant 0, Fig. 5.9 a) shows that it is the

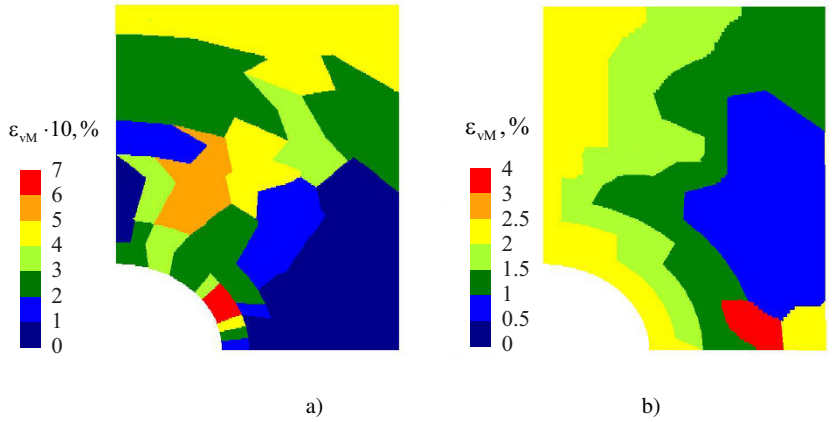

Fig. 5.11: Distribution of the von Mises strains in an aluminum plate with a notch a) thermal and irradiation creep $t_* = 37869$ h, b) thermal, irradiation creep and irradiation swelling, $t_* = 37728$ h.

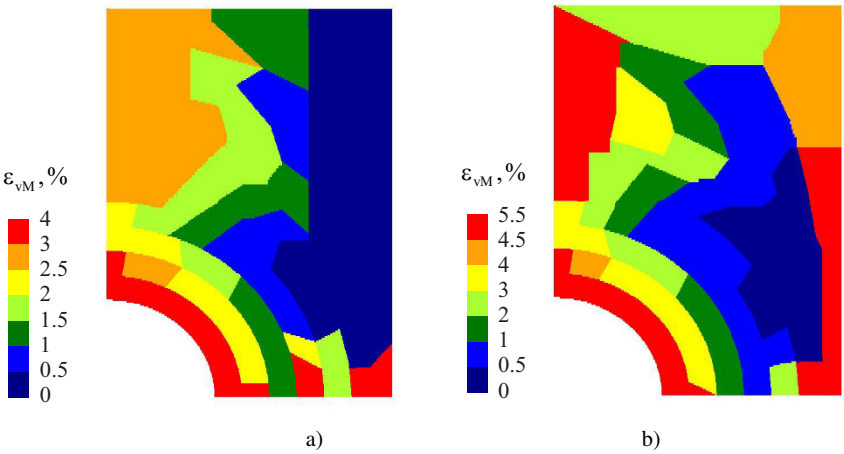

Fig. 5.12: Distribution of the von Mises strains in an aluminum plate with a notch. Thermal, irradiation creep and anisotropic irradiation swelling a) variant 21, $t_* = 50727$ h, b), variant 22, $t_* = 33864$ h.

same as in the classical analysis of creep with damage [6]: zones with significant damage are concentrated near the notch. Adding the influence of radiation taking into account irradiation creep and isotropy of swelling (variant 2, Fig. 5.9 b) significantly intensifies damage in the axial direction. If the swelling properties are considered anisotropic, then due to the higher level of strains and stresses in the axial direction (variant 22, Fig. 5.10 b), the damaged zone increases significantly. We also note that the place of completion of hidden damage accumulation may slightly shift along the edge of the notch.

The effect of radiation on the strain distribution is much greater than on the damage in the plate. This is obviously related to the addition of various mechanisms of deformation growth to the analysis. If, without taking into account radiation exposure, the strains do not exceed 0.01% (variant 0, Fig. 5.8 b), then the combined effect of thermal and irradiation creep (variant 1, Fig. 5.11 a) increases the maximum strain value to 0.7%. The main contribution to the strain level is made by irradiation swelling strains, their maximum is 4-5%.

The distribution along the plate of the maximum strain values also changes qualitatively – from a concentration around the notch in case of thermal creep (variant 0, Fig. 5.8 b) to a significant zone on the sides of the plate in case of radiation creep (variant 1, Fig. 5.11 a) and almost complete significant deformation under the action of irradiation swelling (Fig. 5.11, Fig. 5.12, variants 2, 21, 22). The anisotropy of irradiation swelling changes the location of the zones of maximum strains – now they are located on the sides of the plate, but in variant 22, when the deformation is more intense in the axial direction, their maximum level is greater (5.5%, Fig. 5.12 b). In variant 21, when the higher rate of swelling strains is in the direction perpendicular to the plate axis, due to the mutual influence of stresses, the time to failure is even longer than in case of purely thermal creep. The strain level at the edges of the plate increases significantly, by a factor of two, compared to the isotropic case (variant 2).

Now, we will present the results of the calculations of the deformed state and the distribution of the damage measure when adding a cyclic harmonic loading. We suppose that the stresses in the plate are caused by the cyclic temperature change according to the asymmetry parameter of the heating-cooling cycle H and the motion of the plate edge which is is run according to the harmonic law of traction with the cycle asymmetry parameter L:

$$P = P_0\left(1 + L\frac{2\pi}{T_c}\right), \quad T = T_0\left(1 + H\frac{2\pi}{T_c}\right) \tag{5.14}$$

For numerical modeling, we apply the constitutive equations (5.7) and (5.8). Let us take $L = H = 0.15$. The calculation results are given in Fig. 5.13, which shows the distribution of the damage measure a) and von Mises strains b). The time to the completion of hidden damage accumulation was shorter than in a case with constant stresses. It was equivalent to 28,914 h.

Analyzing the calculation results shown in Fig. 5.13, we come to the conclusion that due to the intensification of the process of damage growth, which ends in the area of the stress concentrator earlier than it was in the case of an unvarying stress field, in the vicinity of the plate far from the concentrator, the values of the damage measure even at η =0.05 are absent (Fig. 5.13 a), as was in the results of variant 2 (Fig. 5.9 b). Due to the shorter time to failure, the overall strain level inside the plate also decreases (Fig. 5.13 b). At the same time, we stress that due to the fact that the strain rate is greater during cyclic loading, their overall level at the edges of the plate becomes the same, 2.5%, in a shorter time , as in purely static processes.

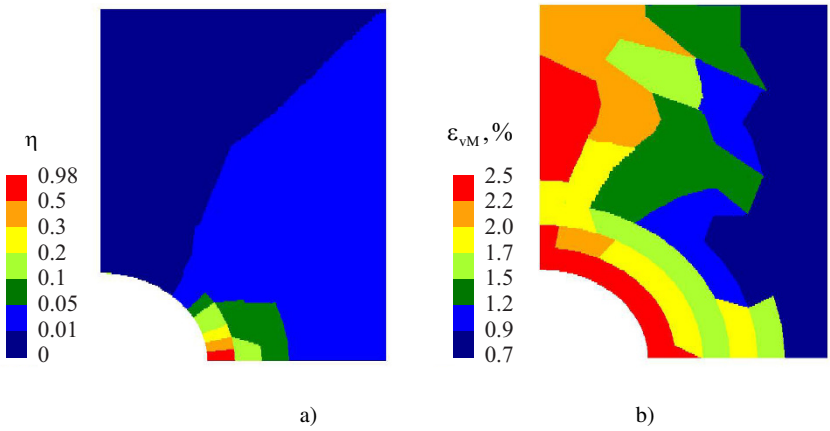

Fig. 5.13: Distribution of the damage measure a) and von Mises strains b) in an aluminum plate with a notch. Cyclic loading. Thermal, irradiation creep and irradiation swelling, $t_* = 28914$ h.

5.5 Conclusions

The approach and method of solving the problems of Creep theory with the application of Continuum Damage Mechanics in the case of action of radiation exposure are considered. The main difference from the classical problems of the Creep theory is the consideration in the analysis of two additional mechanisms of deformation - irradiation creep and irradiation swelling. If the consideration of irradiation creep, which is modeled by a power-law, or quite often even a linear dependence of the strain rate on stresses, does not present difficulties and is easily implemented into the general calculation scheme, then the modeling of irradiation swelling, starting from the construction of the constitutive equation to numerical procedures, is not a standard task. It is not implemented in most software complexes of engineering analysis.

The main problem is the construction of an adequate constitutive equation that reflects the dependence of irradiation swelling deformation on time. It is clear from the point of view of Continuum Mechanics approaches, that the formulation of the equation for the strain rate is better. If such an equation is built and verified, then with the possibility of implementing an additional unit to the FE software tool, the implementation of the calculation method of analysis taking into account the development of volume strains of irradiation swelling will not be a difficult task.

Due to the fact that the evaluation of the processes of joint development in time of thermal and irradiation creep strains, which are also accompanied by the accumulation of hidden damage, together with irradiation swelling strains, an adequate analytical modeling is not possible for the case of a complex stress state with a complex shape of a structural element and boundary conditions. For this, our approach uses a developed calculation method based on a combination of FEM and difference methods of

time integration. A demonstration of the method's capabilities for various cases of deformation and damage of RVI elements is provided for 3D and 2D problems. The possibility of modeling materials with isotropy and anisotropy of long-term material properties, using scalar and tensor parameters of damage, continuing the analysis of fracture after the completion of the accumulation of hidden damage at some point of the element is shown.

The above presented results of calculations show that the contribution of strains caused by radiation exposure of the material in most cases leads to an increase in the overall level of strains and a reduction in the time until the completion of hidden damage. But for the case of materials even with transversal isotropy of properties, due to the contribution of irradiation swelling strains and different nature of stress redistribution in this case, the time to completion of hidden failure may even increase. The addition of a cyclic component of the thermal-force loading in most cases leads to an increase in the overall level of strains and a decrease in the values of time to completion of hidden damage accumulation.

Even with the isotropy of long-term properties, due to the combination of stress relaxation processes during creep and their growth during the growth of irradiation swelling strains with time, it is possible to obtain different dependences of the resulting stress on time, which will affect the time until the completion of hidden failure.

All presented examples show that an adequate analysis of long-term deformation and strength of structural elements exposed to thermal - force and radiation fields is possible only with the use of appropriate calculation tools. Due to the essential nonlinearity of the problems, even a moderate deviation of the parameters can lead to qualitatively different distributions of the components of the stress-strain state. Therefore, the basis of the methods should be adequate and verified constitutive equations, primarily for describing the irradiation swelling strains in time, understanding their isotropic or anisotropic nature.

Acknowledgements Dmytro Breslavsky acknowledges the support by the Volkswagen Foundation within the programme "Visiting research program for refugee Ukrainian scientists" (Az. 9C184).

References

[1] Brumovsky M (2018) Evaluation of Reactor Internals Integrity and Lifetime According to the NTD ASI. In: Proceedings of the ASME 2018 Pressure Vessels and Piping Conference, Pressure Vessels and Piping Conference, vol 1A: Codes and Standards

[2] Chopra OK (2010) Degradation of LWR core internal materials due to neutron irradiation. Argonne National Laboratory, NRC Job Code N6818, Office of Nuclear Regulatory Research

[3] Lee KH, Park JS, Ko HO, Jhung MJ (2013) Analysis for aging and operating experiences of reactor vessel internals. In: Transactions of the Korean Nuclear Society Autumn Meeting Gyeongju, KNS, Daejon

[4] Ma BM (1983) Nuclear Reactor Materials and Applications. Iowa State University
[5] Zinkle SJ, Tanigawa H, Wirth BD (2019) Chapter 5 - radiation and thermomechanical degradation effects in reactor structural alloys. In: Odette GR, Zinkle SJ (eds) Structural Alloys for Nuclear Energy Applications, Elsevier, Boston, pp 163–210
[6] Naumenko K, Altenbach H (2016) Modeling High Temperature Materials Behavior for Structural Analysis - Part I: Continuum Mechanics Foundations and Constitutive Models, Advanced Structured Materials, vol 28. Springer
[7] Ozaltun H, Herman Shen MH, Medvedev P (2011) Assessment of residual stresses on U10Mo alloy based monolithic mini-plates during hot isostatic pressing. Journal of Nuclear Materials **419**(1):76–84
[8] Pandit AM, Blom FJ, Baas PJ (2019) Stress assessment of baffle former bolt of PWR reactor for IASCC. In: 19th International Conference on Environmental Degradation of Materials in Nuclear Power Systems-Water Reactors, Boston, pp 1016–1023
[9] Sangjeung L, Eunho L, NoCheol P, Jongsung K, Youngin C, Jongbeom P (2019) Finite Element Analysis Methodology Reflecting Neutron Irradiation Effects For Structural Analysis. In: Transactions SMiRT-25 (Charlotte, NC, USA, August 4-9, 2019, Division III)
[10] Breslavsky D, Chuprynin A, Morachkovsky O, Tatarinova O, Pro W (2019) Deformation and damage of nuclear power station fuel elements under cyclic loading. The Journal of Strain Analysis for Engineering Design **54**(5-6):348–359
[11] Breslavsky D, Senko A, Tatarinova O, Voevodin V, Kalchenko A (2021) Stress–strain state of nuclear reactor core baffle under the action of thermal and irradiation fields. In: Altenbach H, Amabili M, Mikhlin YV (eds) Nonlinear Mechanics of Complex Structures: From Theory to Engineering Applications, Advanced Structured Materials, Springer, Cham, Advanced Structured Materials, vol 157, pp 279–293
[12] Tonks M, Gaston D, Permann C, Millett P, Hansen G, Wolf D (2010) A coupling methodology for mesoscale-informed nuclear fuel performance codes. Nuclear Engineering and Design **240**(10):2877–2883
[13] Garner FA (2020) Radiation-induced damage in austenitic structural steels used in nuclear reactors. In: Konings RJM, Stoller RE (eds) Comprehensive Nuclear Materials, vol 3, 2nd edn, Elsevier, pp 57–168
[14] Breslavsky D, Tatarinova O, Kalchenko O, Tolstolutska G (2022) Effect of irradiation and thermo-induced processes on reactor in vessel elements during long-term operation. Voprosy Atomnoj Nauki i Tekhniki (2 (138)):3–8
[15] Asundi MK (1961) The role of light metals in nuclear engineering. In: Symposium on Light Metal Industry In India, NML, Jamshedpur, pp 171–179
[16] Garric V, Colas K, Donnadieu P, Loyer-Prost M, Leprêtre F, Cloute-Cazalaa V, Kapusta B (2021) Impact of the microstructure on the swelling of aluminum alloys: Characterization and modelling bases. Journal of Nuclear Materials **557**:153,273

[17] McDonell WR (1972) Irradiation swelling and growth in uranium and other anisotropic metals. Trans Amer Nucl Soc **15**(1)
[18] Dubyk Y, Filonov V, Filonova Y (2019) Swelling of the WWER-1000 Reactor Core Baffle. In: Transactions SMiRT-25 (Charlotte, NC, USA, August 4-9, 2019, Division II)
[19] Yang JS, Lee JG, Oh SJ, Won SY (2015) Irradiation-induced degradation effects on baffle-former-barrel assembly of reactor vessel internal. In: Transactions of the Korean Nuclear Society Spring Meeting reactor vessel internal, KNS, Jeju
[20] Breslavskii DV, Morachkovskii OK (1998) Nonlinear creep and the collapse of flat bodies subjected to high-frequency cyclic loads (in Russ. International Applied Mechanics **34**(3):287–292
[21] Breslavs'kyi DV, Korytko YM, Morachkovs'kyi OK (2011) Cyclic thermal creep model for the bodies of revolution. Strength of Materials **43**(2):134–143
[22] Breslavsky D, Morachkovsky O, Tatarinova O (2014) Creep and damage in shells of revolution under cyclic loading and heating. International Journal of Non-Linear Mechanics **66**:87–95
[23] Breslavsky D, Kozlyuk A, Tatarinova O (2018) Numerical simulation of two-dimensional problems of creep crack growth with material damage consideration. Eastern-European Journal of Enterprise Technologies **2**(7 (92)):27–33
[24] Breslavsky D, Senko A, Tatarinova O (2021) Creep damage and fracture of notched specimens under static and fast periodic loading. International Journal of Damage Mechanics **30**(6):964–983
[25] Breslavsky DV, Korytko YN, Tatarinova OA (2017) Design and development of finite element method software (in Ukrain.). Pidruchnyk NTU KhPI
[26] Breslavsky DV (2020) Deformation and Long Term Strength of Structural Elements of Nuclear Reactors. Madrid, Kharkiv
[27] Morachkovsky OK, Pasynok MA (1997) Creep of isotropic and anisotropic plane bodies (in Russ.). In: Proceedings of International Scientific and Technical Conference "Information Technologies: Science, Engineering, Technology, Education, Health", vol 1, Kharkiv State Polytechnic University, Kharkiv, pp 127–131
[28] Altenbach H, Breslavsky D, Mietielov V, Tatarinova O (2020) Short term transversally isotropic creep of plates under static and periodic loading. In: Naumenko K, Krüger M (eds) Advances in Mechanics of High-Temperature Materials, Springer, Cham, Advanced Structured Materials, vol 117, pp 181–211
[29] Farrell K, King R, Jostsons A (1973) Examination of the irradiated 6061 aluminum hfir target holder. Oak Ridge National Lab., Tenn.
[30] Galishin AZ, Sklepus SN (2019) Prediction of the time to failure of axisymmetrically loaded hollow cylinders under conditions of creep. Journal of Mathematical Sciences **240**(2):194–207
[31] Frost BRT (2013) Nuclear Fuel Elements: Design, Fabrication and Performance. Elsevier
[32] Konkin VN, Morachkovskii OK (1987) Creep and long-term strength of light alloys with anisotropic properties. Strength of Materials **19**(5):626–631

[33] Aitkhozhin ES, Chumakov EV (1996) Radiation-induced creep of copper, aluminium and their alloys. Journal of Nuclear Materials **233-237**:537–541